GROUND DISPLACEMENT AFTER MW6.7 EARTHQUAKE IN LAKE KHÖVSGÖL OF MONGOLIA DETERMINED SENTINEL-1B SATELLITE DATA

Zolzaya Lkhamsuren[1*, 2], Liu Da Wei[1], Ochirkhuyag Lkhamjav[2], Bayartungalag Batsaikhan[2]

[1]Graduate Student of Master Program of Remote Sensing and Geographic Information System in Beijing Aerospace and Astronautic University, Email: zolzayamust@gmail.com, david_liu863@126.com

[2] Mongolian Geo-Spatial Association, Email: info@geomedeelel.mn

KEY WORDS: Sentinel1B, Earthquake, Ground displacement, Deformation, Interferometric, SAR

ABSTRACT: Conventional field-based monitoring or large-scale monitoring is a costly and time-consuming process that requires many days, people and equipment in different field weather conditions. According to the remote sensing-based satellite data, which is the main advanced technology of modern science, it is economical and stable without requiring brigade manpower and special equipment, regardless of time and space location, without visiting the area for research and analysis. There are two main methods of traditional measurement and radar remote sensing to study ground deformation and displacement such as subsidence, uplift, and horizontal and vertical displacement. This study's purpose is to monitor for ground deformation and displacement before after the earthquake using a kind of SAR satellite of remote sensing-based on Differential Interferometric Synthetic Aperture Radar technology recently happened earthquakes in Mongolia. In this research has selected as the study area for happened earthquake epicenter magnitude 6.7 north centered of Khövsgöl Lake 26 km distanced from western south of Turt soum local time when at the 05:30 am 12th of Jan, 2021. As a result of the study, when mapping the scatters of ground displacement impacted after earthquake epicenter depth of Khövsgöl lake around was defined surface subsidence -22 cm where on two-part section ground with between 7.2 km distance, located until about 15km from steep to the west the lakeside.

1. INTRODUCTION

Measuring and determining landslide deformation helps to gain a deeper understanding of natural phenomena and their interrelationships, such as earthquakes [1], volcanic eruptions, landslides, and landslides [2,3], thereby reducing the risk of natural disasters and preventive policy management. It is also important in determining the impact of issues such as underground engineering and mining and underground mining, groundwater use, dam and flood protection management, structural instability of buildings, and subsidence [8]. There are two main methods of traditional measurement and remote sensing to study land deformation, such as subsidence, elevation, and horizontal and vertical displacement. Conventional or field-based measurement or large-scale monitoring and analysis is a costly and time-consuming process that requires many days, many people, labor, and equipment in different field weather conditions. Brigade manpower and special equipment, regardless of time and space, without remote sensing based on remote sensing-based satellite data, which is the main advanced technology of modern science. It has the advantage over area measurement in that it can be carried out in an economical manner without requiring it, and that the same results can be achieved by performing stationary processing.

There are two main types of satellite data: optical and radar. Of these, optical satellite data depends on weather conditions, the atmosphere, and the effects of visible light radiation. The reflected light is recorded on the radar antenna, so it has the advantage of being able to map smoothly in any weather conditions, such as day and night, cloudy and overcast [5]. The Sentinel-1B satellite transmits shortwave frequencies of 5.405 GHz on a radar antenna in the C channel (5.55 cm) region.

The purpose of the research

The purpose of this study is to use the Sentinel1-B satellite data for InSAR processing on SNAP software to show how seismic changes in the vicinity of the study area are caused by strong earthquakes in a short period of time.

Study area and data set

Earthquake-induced deformation remains one of the most important issues in many fields of science. Regular monitoring and measurement of pre-earthquake and post-earthquake deformation provides a wealth of information on earthquake risk reduction, as well as valuable insights into the stages of surface deformation accumulation and seismic properties [4].

According to seismic data for the last 10 years, there have been 237,647 earthquakes in the territory and border areas of Mongolia, of which 1,271 were earthquakes with a magnitude of more than 3.5. The western region accounts for more than 80 percent of all traffic in Mongolia. In the last 5 years, there have been 295 recent earthquakes with a magnitude of more than 3.5 in Mongolia and neighboring regions, and more than 54 in the Western region. There have been 10 earthquakes with a magnitude of more than 5.0 in the Western region since 2011. [11]

The most recent 6.7-magnitude tremor was recorded in the center of Khövsgöl Lake. Data from 9 channel routes were compiled and used in the IW2 track (Figure 1).

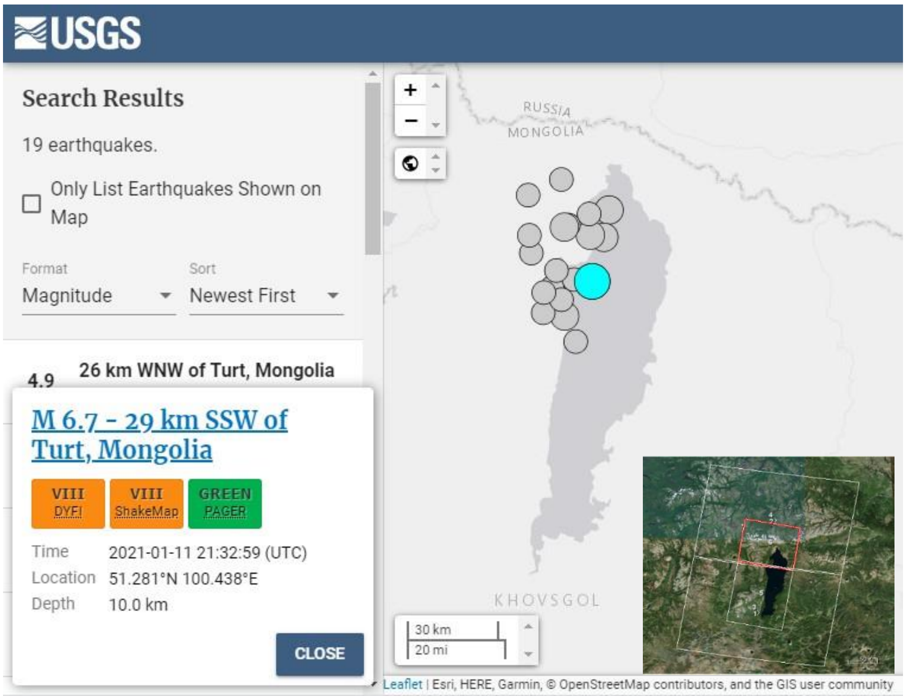

Figure 1. A map of the location of a 6.7 magnitude earthquake in Khövsgöl province [16] shows an area containing data on the orbital numbers, 24880 and 25230, of the Sentinel-1B satellite IW mode transmission-Descending, Polarization-VV, VH.

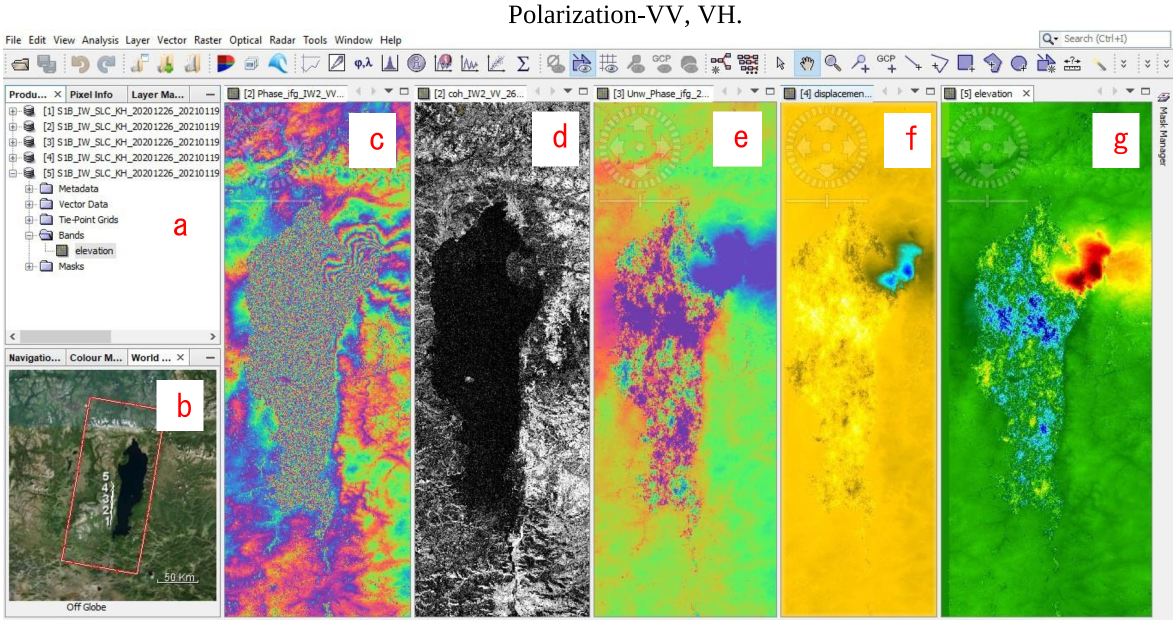

Figure 2. SNAP 8.0 software workspace and data processing steps

a. A window containing satellite channel information
b. Location map of the data being processed
c. Phase interferometer phenomenon
d. Wave phase coherent compatibility map
e. Phase filtering
f. The result that describes the transition
g. Results include elevation

2. APPROACHES

Differential Interferometer Synthetic Aperture Radar (DInSAR) calculates ground deformation and ground displacement based on the phase difference of the radar data interferometer recorded at least two or more times at different times in the same area （including DEM) [1]. Landslides can occur as a result of changes in geological faults or as a result of strong earthquakes and volcanic activity.

The SentiNEl Application Platform (SNAP) 8.0, an open source software developed by the European Space Agency, is a comprehensive system for processing SAR (Synthetic Aperture Radar) type satellite data. Performs step-by-step processing according to and displays the resulting figure on the screen (Figure 2). This means that the process is automated based on the following mathematical calculations and the results are shown.

Spatial geometry and mathematical processing

Assuming that there is a single dominant scattering point in each cell of the surface density (ground resolution cell） two SAR satellite images are observed from two different angles, as shown in Figure 3 [1].

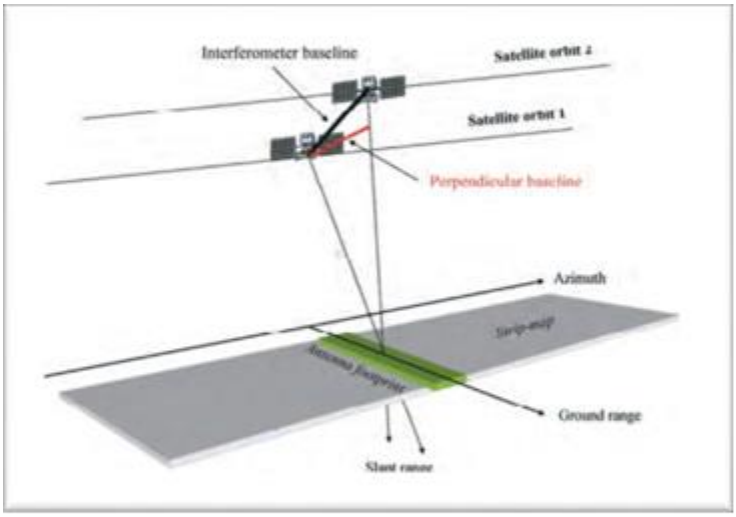

Figure 3: Geometric representation of a satellite interferometer with SAR system

The distance between the orbits of a satellite is called the base line of the interferometer, and the main parameter of the interferometer is projected perpendicular to the direction of its slope (slant range) [1]. In this case, the interferometer phase of each pixel in the SAR image depends only on the difference in the length of the path from the two satellites to the point at the location (Figure 4) [10].

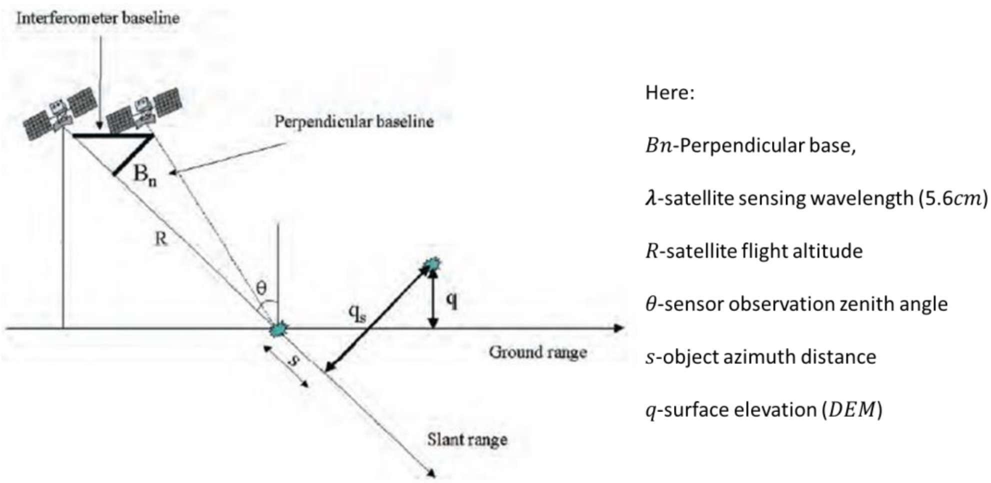

Figure 4. Geometric principles for measuring surface changes

If we approximate the difference in flight altitude, the formula is written as follows.

$$\Delta r = -2\,\frac{B_n\, q_s}{R} \qquad (1)$$

From this we can find the phase difference of the surface transition, and the phase variation ($\Delta\phi int$) of the interferometer is proportional to Δr divided by the transmitted wavelength (λ), and the formula for finding the phase difference can be written as.

$$\Delta\phi = \frac{2\pi\Delta r}{\lambda} = \frac{4\pi}{\lambda}\frac{B_n\, q_s}{R} \quad (2)$$

The phase variability of the interferometer depends on two conditions

1. The q between the observation point defined in the horizontal plane and the change in height 2 is proportional to the phase fluctuation.

2. Assuming that the displacement of the observation point S is proportional to the phase fluctuation in the slope, the formula is given by

$$\Delta\phi = -\frac{4\pi}{\lambda}\frac{B_n\, q}{R\sin\theta} - \frac{4\pi}{\lambda}\frac{B_n\, s}{R\tan\theta} \quad (2.1)$$

The total phase difference is calculated as the sum of the altitude model and the global plane rotational correction, the surface transition phase, the atmospheric correction of the initial data and repeat flight in the satellite area, and the noise correction of the wave transmission.

$$\Delta\phi_{int} = (\Delta\phi_{dem} + \Delta\phi_{flat}) + \Delta\phi_{defo} + \Delta\phi_{atm} + \Delta\phi_{noise} \quad (3)$$

When the formula is decomposed, it is written as follows. [7]

$$\boxed{-\frac{4\pi}{\lambda}\frac{B_n S}{R\tan\theta}}\ \boxed{-\frac{\Delta q}{\sin\theta}\cdot\frac{B_n}{R_0}\cdot\frac{4\pi}{\lambda}}\ \boxed{+\frac{4\pi}{\lambda}d} \quad (3.1)$$

Here, $\Delta\phi_{int}$ = interferogram phase difference

$\Delta\phi_{flat}$ = phase difference due to the plane of the earth

$\Delta\phi_{dem}$ = phase difference due to elevation

$\Delta\phi_{defo}$ = phase difference due to land deformation and displacement

$\Delta\phi_{atm}$ = phase difference due to the atmosphere

$\Delta\phi_{noise}$ = phase difference due to noise

From this, we calculate the phase difference of the interferometer based on the coherence of the wavelength of the satellite data wave or two image pixels that have flown two or more times in the same orbit, in terms of orbital correction, atmospheric correction, numerical model of surface elevation, and noise. can accurately determine surface deformation. [7]

$$\Delta\phi_{defo} + \Delta\phi_{atm} + \Delta\phi_{noise} = \Delta\phi_{int} - \Delta\phi_{dem} - \Delta\phi_{flat} \qquad (3.2)$$

This study determines the relative deformation of the surface and does not require the many hours of processing required for time series analysis, it was performed step-by-step according to the following flowchart using the SNAP software command tools (Figure 5).

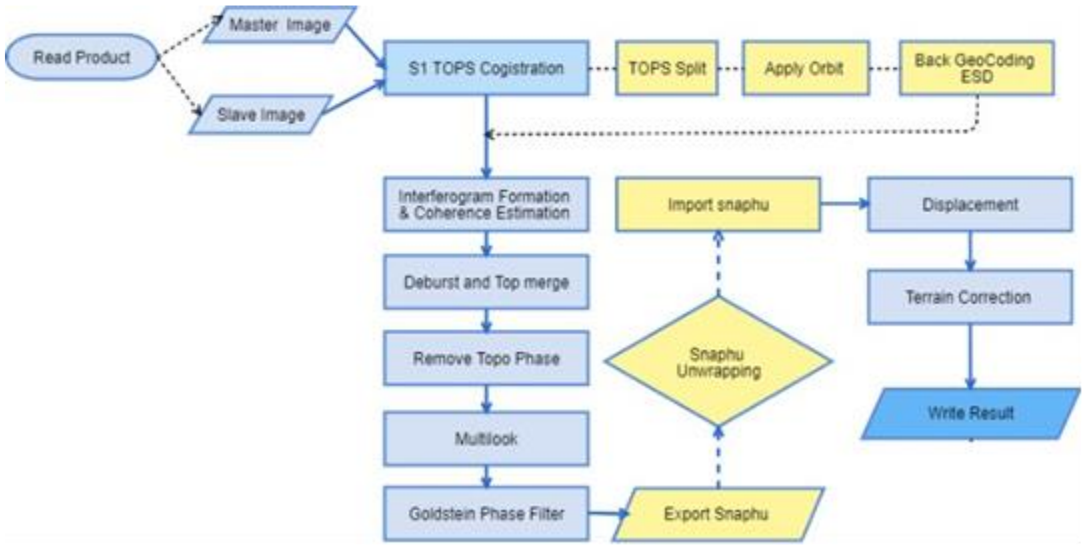

Figure 5. Image processing flow chart to determine ground movement by InSAR satellite data

3. RESULTS

When finding the phase difference of the differential interferometer of the two images taken before and after the earthquake using Equation 3.2, the relationship between the master and slave data of the observed area is very important. In other words, the difference in interferometry is also largely due to seasonal conditions in the study area, such as snow and ice cover, its thick vegetation cover, and thickening.

The two images are not too far apart, the snow depth is close, and there is no change in freezing and thawing, no rain or flood water, no air temperature, no surface precipitation, and noisy wind speed during the transmission of its thickness ($\Delta\phi atm$). It is recommended to process two data obtained under the same conditions as possible, as they may vary slightly depending on the degree of $\phi noise$). [7]

Accordingly, the selected 2-day weather forecast was submitted to the Information And Research Institute Of Meteorology, Hydrology And Environment (IRIMHE) based on the official requested, in writing, and the air temperature difference (-1-2 temperature), the difference in precipitation thickness (-1 cm) and the change in wind speed were about -2 m/s, and it is concluded that these are not conditions that can affect the result of surface deformation (Table 1).

Table 1. Weather information in the study area*

Date	**Temperature (^{0}C)**		**Wind directions and speed (m/s)**	**Precipitation (cm)**
	Day	**Night**		
2020-Dec-26	-18-22	-25-32	NW, 4-9 m/s	0-14 cm, snow
2021-Jan-19	-19-24	-27-32	SW, 6-11 m/s	0-13 cm, snow

**Source: IRIMHE data*

The image is processed step by step and the interrelated results are exported in raster format (geotiff) and overlapped with other geological images and elevation in the geographic information system's ArcGIS software (Figure 6), and based on the figure 6, the following hypothesis is made.

Observations of the location of the epicenter showed that the vertical displacement or subsidence at the study site overlapped on a 1: 200,000 scale geological map. The undeveloped mainland rift at the lower end of the seven-million-year-old Doloon Mountain may have been flattened by the Neogene olivine priocent basalt ($\beta N1$), the glacial end moraine gravel, sandstone, and loam ($gdQ3$).

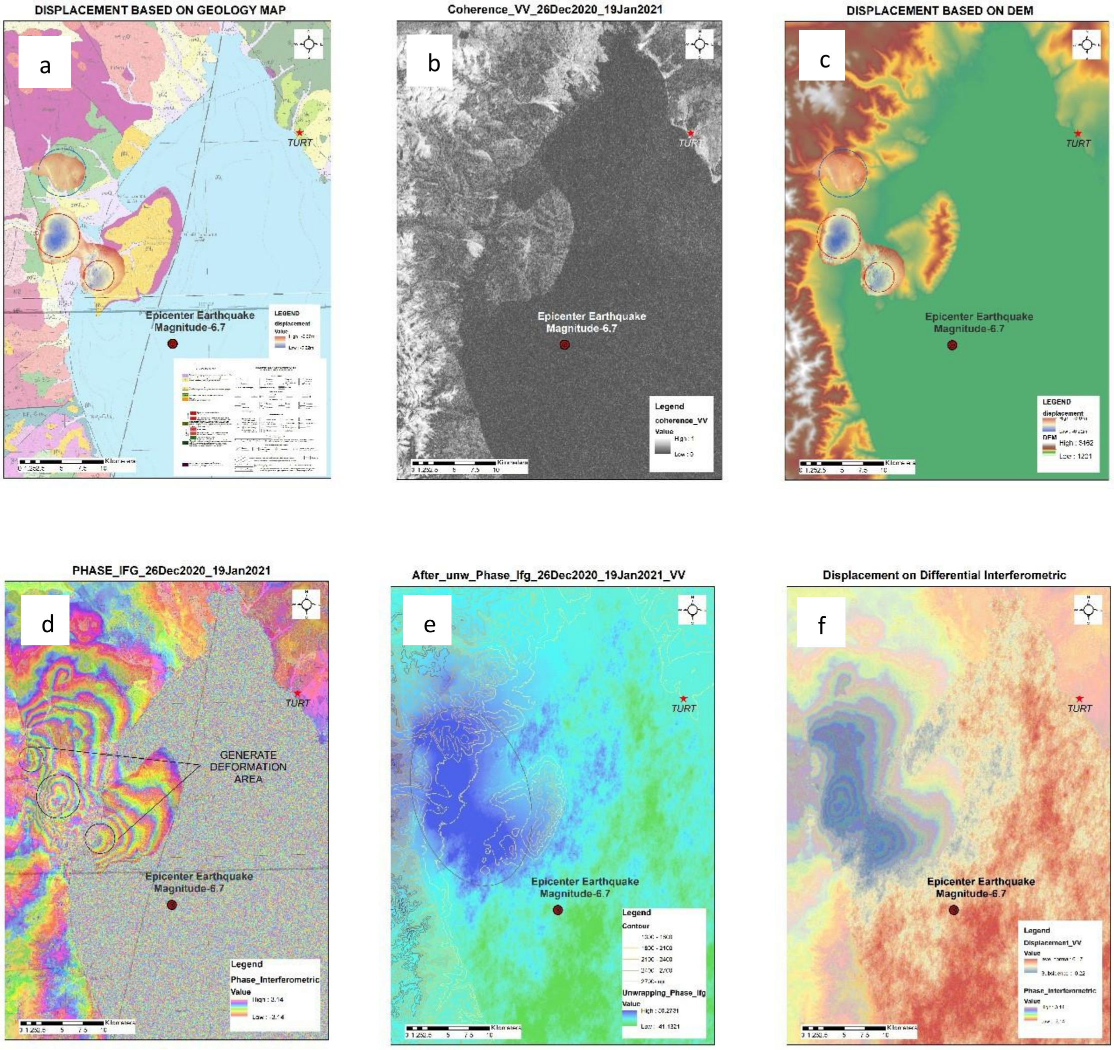

Figure 6. Overlap of processing images shown in the vicinity of the subsidence with other data

(a) Overlap of the displacement on the geological background map (b) Wave propagation combination
(c) Overlap of the displacement on the DEM (d) Differential interferometer phase formation
(e) Phase-filtered image (f) Transition phase overlap

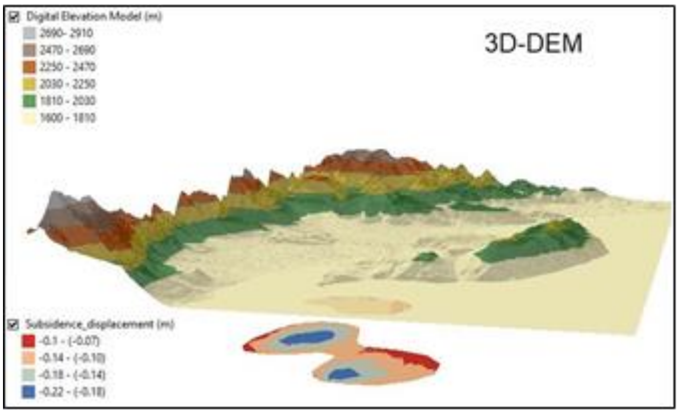

Figure 7. The seismic or vertical displacement in the northwestern part of Khövsgöl Lake (18 -22 cm) caused by the earthquake is shown in 3D on the DEM.

It is always necessary to compare a research paper with an analysis developed in a different way. Furthermore, the results show a quantitative model of elevation based on its own resources, as it was not possible to conduct geodetic and geodynamic measurements in the depths of the lake in winter during the earthquake.

In addition, the Institute of Astronomy and Geophysics of the Mongolian Academy of Sciences (MAS) presented two different types of research results in an e-learning course dedicated to the "Earthquake Prevention and Awareness Day" on March 24, 2021. Note that the same results were obtained. [9]

1. The study of the epicenter mechanism examines how the expansion of seismic boundaries depends on the zone of expansion and contraction. The decline is shown in Figure 8
2. Confirming the above mechanism, the Institute's expert described the interferometer image developed by InSAR satellite data from two pre- and post-earthquake data as a vertical shift of about -30 cm on the west coast of the Khövsgöl Lake (Figure 9).

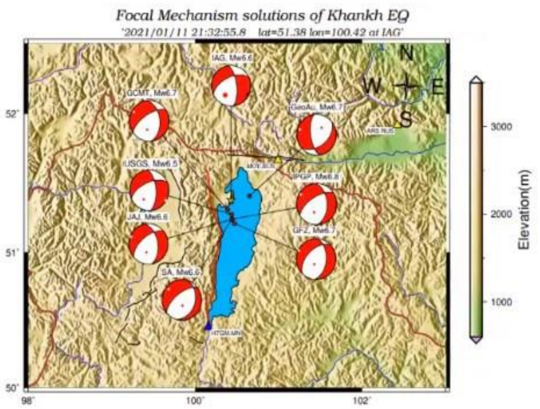

Figure 8. Focal Mechanism in the study area Source: D.Ganzorig, IAG

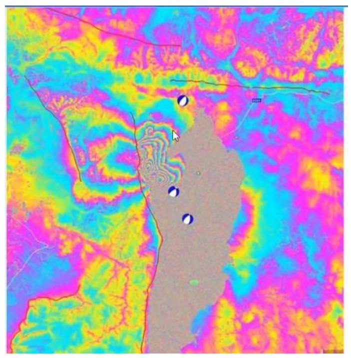

Figure 9. InSAR image Source: E.Bayarsaikhan, IAG

Impact and risks of landslides:

During the earthquake, the quake was felt not only in Khuvsgul aimag, but also in soums and neighboring western aimags, for example, a resident of the 14th floor of Khuushiin Am in Khan-Uul district of Ulaanbaatar felt nauseous and felt the feeling of packing in a horizontal position. . A resident of the 11th district of Baga Toiruu, Sukhbaatar district, felt a throbbing heartbeat [Social Media information].

In these cases, the seismic strength may have varied depending on the geology, geomorphology, subsidence, and elevation of the site, as well as the seismic resistance of the structure, materials, and quality.

4. CONCLUSION

In this study, the relative changes in the selected area, or changes in the surface in a short period of time, were graphically represented. As a result of the survey, a 6.5 magnitude earthquake in the center of Lake Hövsgöl caused landslides 10-15 km to the west of the northwestern shore of the lake and -18-22 in two areas about 8 km apart in the vertical direction. cm of subsidence.

Time Series Analysis and how the distribution will continue in the future. The Persistent Scatterer Interferometry is being developed for in-depth study.

Acknowledgements

We would like to thank E. Bayarsaikhan, the Institute of Astronomy and Geophysics, Mongolian Academy of Sciences, A, Sumiya, the Agency of Land Management, Geodesy and Cartography, A. Braun, moderator of the ESA Forum, for their assistance in the analysis of the development process, and Professor Liu Da Wei of Peking University of Aerospace, who provided general information on the topic and related research.

5. REFERENCES

Alberto Moreira, Pau Prats-Iraola, Marwan Younis, Gerhard Krieger, Irena Hajnsek and Konstantinos P. Papathanassiou. 2014, Microwaves and Radar Institute of the German Aerospace Center (DLR), Germany Alberto Moreira., Tutorial on Synthetic Aperture Radar., 21 May 2014.

Braun. A L. Veci. 2021, TOPS Interferometry Tutorial Sentinel-1 Toolbox link: http://step.esa.int/docs/tutorials/S1TBX%20TOPSAR%20Interferometry%20with%20Sentinel-1%20Tutorial_v2.pdf

Chen Y., Zhang G., Ding X., et.al 2001, Monitoring Earth Surface Deformations with InSAR Technology: Principle and some Critical Issues [J]. Journal of Geospatial Engineering, 2:3–21.

"Earthquake Prevention and Awareness Day" e-learning presentation. https://www.facebook.com/watch/?v=832322370690079

European Space Agency. 2007, InSAR Principles: Guidelines for SAR Interferometry Processing and Interpretation. TM-19A, B. Feb-2007., (A-3: A-17)

Huang Lin Chao. 2016, Ground Displacement Detection of La Paz City based on Satellite Interferometric Synthetic Aperture Radar (InSAR), A Dissertation Submitted for the Degree of Master, BUAA, 2016

Liu P., Li Z., and Hoey T. 2013, Using advanced InSAR time series techniques to monitor landslide movements in Badong of the Three Gorges region, China [J]. International Journal of Applied Earth Observation and Geoinformation, 2013, 21:253–264.

Sumiya, A 2020, Sentinel-1 Satellite Data Determination of Urban Activity, Deformation of Buildings and Structures. ESH, 2020

Synthetic Aperture Radar Land Applications Tutorial. Part I Background and Theory. Prepared by ESA SARmap UNESCO https://earth.esa.int/documents/10174/2700124/sar_land_apps_1_theory.pdf

Yehia H. Miky. 2019, Multitemporal Sentinel-1SAR Interferometry for Surface Deformation Monitoring near High Dam in Aswan, Egypt, American Journal of Geographic Information System, Vol. 8 No. 2, 2019, pp. 96-102.

Zagdsuren.S, Diimaa. B, Batbayar. P, Ganzorig. Kh, Mungunkhuu. Ch and Chimedtseren. P 2017, Earthquake Mode Study (Khovd). Khovd branch of the Institute of Astronomy and Geophysics of the Mongolian Academy of Sciences https://iag.mn/file/Journals/Geophysics_and_Astronomy_2017_4.pdf